Ultrafast Photon-Photon Interaction in a Strongly Coupled Quantum Dot-Cavity System

Dirk Englund,[1,2,*,†] Arka Majumdar,[1,†] Michal Bajcsy,[1] Andrei Faraon,[1] Pierre Petroff,[3] and Jelena Vučković[1]

[1]*E. L. Ginzton Laboratory, Stanford University, Stanford, California, 94305, USA*

[2]*Department of Electrical Engineering and Department of Applied Physics, Columbia University, New York, New York 10027, USA*

[3]*Materials Department, University of California, Santa Barbara, California 93106, USA*

(Received 15 July 2011; revised manuscript received 28 December 2011; published 2 March 2012)

We study dynamics of the interaction between two weak light beams mediated by a strongly coupled quantum dot–photonic crystal cavity system. First, we perform all-optical switching of a weak continuous-wave signal with a pulsed control beam, and then perform switching between two weak pulsed beams (40 ps pulses). Our results show that the quantum dot–nanocavity system enables fast, controllable optical switching at the single-photon level.

DOI: 10.1103/PhysRevLett.108.093604 PACS numbers: 42.50.−p, 42.65.−k

Techniques enabling efficient interactions between single photons and quantum emitters are fundamental to the field of quantum optics. At the same time, optical nonlinearities at a single-photon level may enable ultralow power and high-speed all-optical gates and switches for classical optical information processing [1,2]. Recent experiments have shown that the necessary nonlinearity may be realized using atomic gases in the slow light regime [3] or solid-state systems consisting of a single quantum dot (QD) strongly coupled to a nanocavity [4–6]. To estimate the speed of such switching in the solid-state approach, we describe here the time-resolved dynamics of light interacting with the QD-cavity system. We first study the interaction of a weak continuous-wave signal and a pulsed control, and then the interaction of two weak (40 ps) laser pulses.

The experiment is performed using a QD strongly coupled to three-hole (L3) photonic crystal (PC) cavity [7], superposed with a grating to increase the emission directionality [8] [see Fig. 1(a)]. The cavity was fabricated in a 160 nm thick membrane containing a central layer of self-assembled InAs QDs with a density of $\sim 50/\mu\mathrm{m}^2$ and an inhomogeneously distributed emission at 925 ± 15 nm.

The eigenfrequencies $\omega_\pm$ of a system consisting of a cavity and a coupled QD are

$$\omega_\pm = \frac{\omega_r + \omega_d}{2} - i\frac{\kappa + \gamma}{2} \pm \sqrt{g^2 + \frac{1}{4}(\delta - i(\kappa - \gamma))^2}. \tag{1}$$

Here, the system is modeled with a Jaynes-Cummings Hamiltonian, where ω_r and ω_d are the cavity and QD resonance frequencies, respectively, κ and γ are the cavity field decay rate, and QD dipole decay rate, g denotes the coherent interaction strength between the QD and the cavity field, and $\delta = \omega_d - \omega_r$ is the QD-cavity detuning. The parameters of the emitter-cavity system used in the experiment [obtained by fitting the spectrum of coupled QD-cavity system at resonance as shown in Fig. 1(d)] are $g/2\pi = 25$ GHz and $\kappa/2\pi = 27$ GHz. The spectrum of the coupled QD-cavity system does not depend strongly on the QD dipole decay rate γ, as it is much smaller compared to g and κ. However, this parameter is estimated from the time-resolved measurements of the uncoupled QD emission and from QD linewidth measurements in off-resonant dot-cavity coupling [9] to be equal to $\gamma/2\pi \sim 1$ GHz. For these parameters, the expression under square root in Eq. (1) is positive for $\delta = 0$, implying that the system is in the strong coupling regime of the cavity quantum electrodynamics (QED).

We characterize the system in a cross-polarized confocal microscope setup in a He flow cryostat [Fig. 1(b)]. The photoluminescence (PL) scans in Fig. 1(c) show the anticrossing between the QD-like states and the cavitylike states as the temperature is raised from 36 to 42 K, giving the polariton energies given by Eq. (1). The cavity transmission, obtained using a broadband light source at 930 ± 20 nm in the cross-polarized configuration [4] shown in Fig. 1(b), shows the same mode splitting in Fig. 1(d). We also characterize the system by time-resolved photoluminescence after the QD is quasiresonantly excited with 3.5 ps pulses at 878 nm. As shown in Fig. 1(e), the PL decays with a characteristic time of 17 ps, as measured using a streak camera with 3 ps timing resolution. This decay closely matches a theoretical model of the cavity field and coupled QD system, as described in the Supplemental Material [10]. Very weak above-band laser power (1 nW measured before the objective lens) is used in this measurement, in order to avoid the generation of multiexcitonic complexes which may affect the measured lifetime [11].

The coupled QD-cavity system enables a strong interaction between two weak laser fields. This was previously demonstrated for two slightly frequency detuned continuous-wave (CW) beams [6]. However, for practical applications of this effect, it is important to demonstrate such interaction with ultrafast optical pulses. Moreover, for practical applications it is critical that signal and control

beams are at the same frequency, in order to enable cascading of the switches [12]. In both experiments presented below we used signal and control beams of the same frequency. (In the Supplemental Material [10], we present switching results for slightly detuned CW and pulsed beams). We first study the time-resolved dynamics of this interaction between CW "signal" and pulsed "control" beams, both within the linewidth of the cavity resonance. In the experiment, with the QD resonant with the cavity and the control and signal beams tuned to the bottom of the transmission dip [shown in Fig. 1(d)], we measure the time-resolved transmission of the control $T(c)$, the signal $T(s)$, and the signal and control $T(s+c)$ on the streak camera. The system temperature is set to 30 K for this experiment. This measurement was taken on the same system from Fig. 1, but on a different day when the QD cavity became resonant at lower temperature than in Fig. 1(c).

We first set the signal and control fields resonant with the tuned QD-cavity system and attenuate the power so that the average intracavity photon number is nearly zero; this corresponds to 12 nW for the CW beam and ~0.2 nW average power for the pulsed control (40 ps pulses, 13 ns repetition period), both measured before the objective lens. Considering a coupling efficiency into the cavity of $\eta \sim 3\%$ [4], this corresponds to an average intracavity photon number of $\langle a^\dagger a \rangle \sim 0.005$ for the CW signal beam and up to 0.025 (per pulse) for the pulsed control beam. Here the intracavity photon number is estimated as $\eta P_{\text{in}}/(2\kappa\hbar\omega_r)$ for the CW beam, where P_{in} is the average input power measured before the objective lens [4]. For a pulsed beam this expression is multiplied by a factor 325, corresponding to the ratio between the repetition period and the pulse duration. In the following figures $\langle a^\dagger a \rangle$ corresponds to the instantaneous cavity photon number. Figure 2(a), panel 1, plots the curves $T(c)$, $T(s)$, $T(s+c)$, as well as the difference $\Delta T = T(c+s) - T(c) - T(s)$, which provides a measure of the nonlinear response of the system. Measurements for two additional sets of curves with higher powers in signal (168 nW and 240 nW, respectively) and control (1.6 and 3.8 nW, respectively), are shown in panels 2 and 3 of Fig. 2(a). We observe that the difference ΔT increases with increasing laser power, as the QD is driven closer to saturation. We note that, for the three sets of data, the collection efficiency and integration time of collection are different, due to

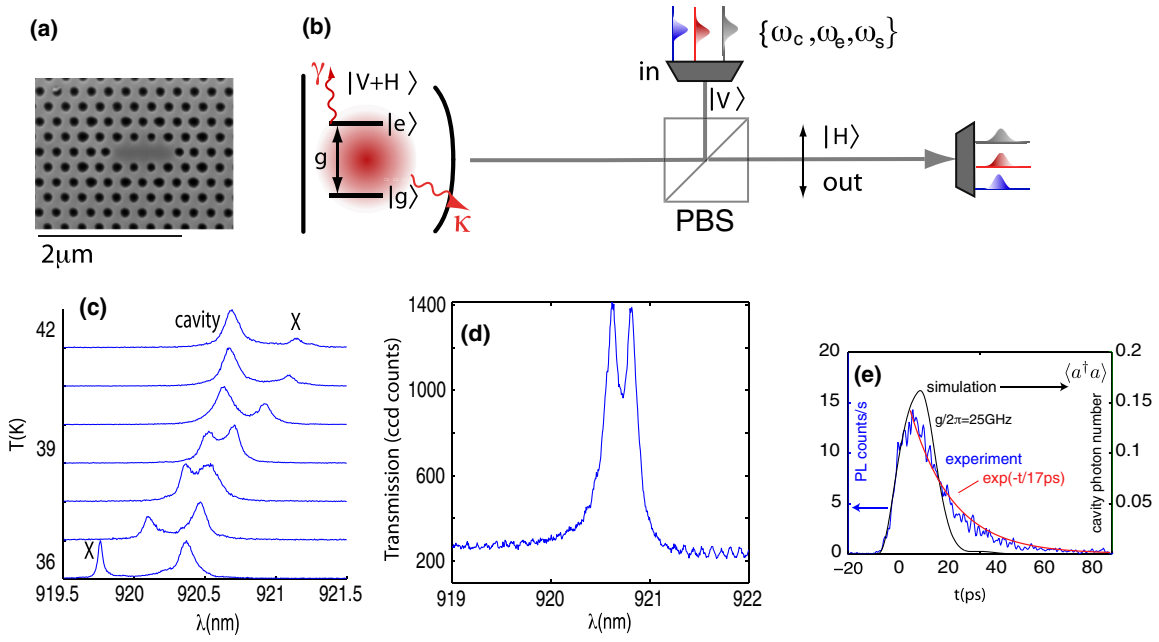

FIG. 1 (color online). (a) Scanning electron micrograph of the photonic crystal cavity. (b) In the experiment, a combination of pulsed control laser (frequency ω_c), nonresonant pulsed or continuous-wave pump laser at ω_e above the QD exciton line, and pulsed or continuous-wave signal laser (ω_s) is employed. The cavity is backed by a distributed Bragg reflector, effectively creating a single-sided cavity [4]. A cross-polarized confocal microscope configuration reduces the laser background that is reflected from the sample without coupling to the cavity, which is polarized at 45° to the incident laser polarization. The measurement is effectively a transmission measurement from the horizontal (H) into the vertical (V) polarization. (c) Anticrossing observed in the PL as the QD single exciton (X) is temperature tuned through the cavity. The QD is pumped through higher-order excited states by optical excitation at ω_e corresponding to a wavelength of $\lambda_e = 878$ nm. (d) The transmitted intensity of a broadband light source (in the cross-polarized setup) shows the mode splitting of the strongly coupled QD-cavity system (this signal is resolved on a spectrometer). (e) PL lifetime ~17 ps when the QD is tuned into the cavity and pulsed excitation is at wavelength $\lambda_e = 878$ nm. The emission that is expected theoretically, based on the system parameters in (d) and a 10-ps relaxation time into the single exciton state, is shown in the solid line.

mechanical instability of the system. A stochastic simulation of the quantum master equation (see the Supplemental Material [10]) yields the cavity transmission, which is proportional to the intracavity photon numbers $n(c)$, $n(c+s)$, and $n(s)$, as well as the nonlinear signal Δn, all plotted in Fig. 2(b) and showing good agreement with the experiment in Fig. 2(a). In fitting the data, the intensities of the pulsed and CW beams were not free parameters, but were fixed by the experimentally measured optical powers, using the same coupling efficiency η. We note that in these simulations we did not include the effect of pure QD dephasing [13], as the role of these particular simulations is to just qualitatively show the expected system dynamics. However, we do include the effect of dephasing in the simulations of the actual optical switching between two pulses described below. As previously reported [14], dephasing reduces the switching contrast, which can be alleviated by performing the experiment at lower temperature.

Finally, we perform the actual all-optical switching experiment between two weak, 40 ps optical pulses, by interacting them in a strongly coupled QD-cavity system. The pulses are resonant with the cavity and have a relative delay of Δt. The pulse pair is generated using the delay setup of Fig. 3(a). The pulses are therefore at the same frequency, but to eliminate interference between the two pulses, we detune them by 40 MHz and average measurement over many pulse pairs (this detuning is very small compared to the pulse bandwidth). Same as in the experiments in Fig. 2, numerical integration of the master equation predicts an increased transmission when both pulses are simultaneously coupled to the cavity. This is shown for a particular choice of powers in Fig. 3(b).

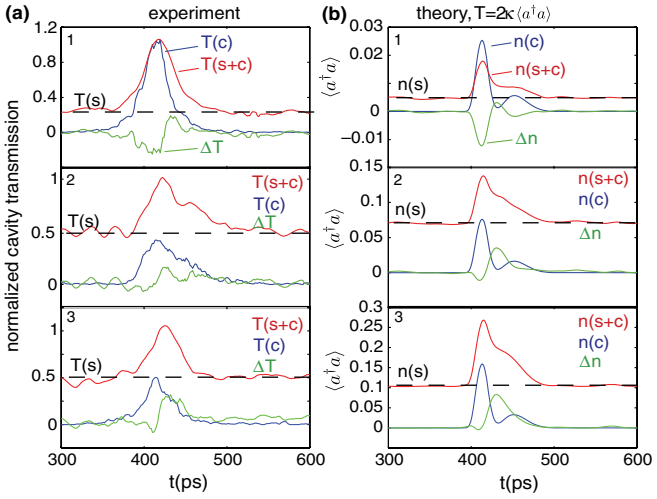

FIG. 2 (color online). All-optical switching of the CW signal beam by a pulsed control beam through the strongly coupled QD/cavity system. (a) Cavity transmission when the signal and control are tuned to the cavity, which is resonant with the QD (panel 1). The transmitted cavity output is normalized with respect to the maximum cavity transmission. As the signal and control input powers are increased (panels 2 and 3), the QD saturates and results in a net-positive nonlinear transmission. For the three panels, the CW signal powers are 12, 168, and 240 nW, respectively; the pulsed control powers are 0.2, 1.6, and 3.8 nW, respectively (all measured before the objective lens). (b) Plots of the theoretically estimated intracavity photon number $\langle a^\dagger a\rangle$, which gives the transmission by $T = 2\kappa\langle a^\dagger a\rangle$. We plot the calculated intracavity photon number for the control beam intracavity photon number $n(c)$, signal and control $n(s+c)$, and the differential photon number $\Delta n = n(s+c) - n(s) - n(c)$.

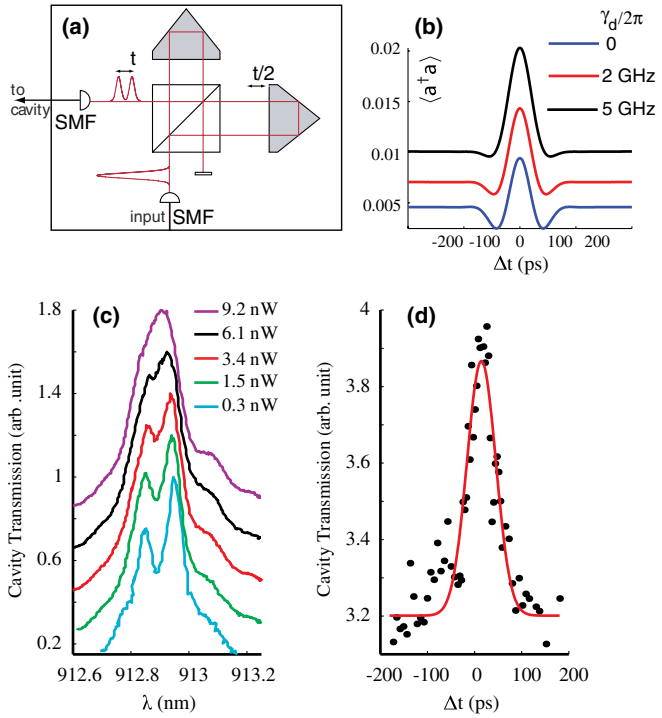

FIG. 3 (color online). All-optical switching between two weak laser pulses interacting via a strongly coupled QD-cavity system. (a) Time-delay setup for producing pulses at a separation of Δt. (b) Simulated interaction of two laser pulses, represented by the instantaneous intracavity photon number $\langle a^\dagger a\rangle$ as a function of the time delay Δt between the two 40 ps long Gaussian pulses. Curves are calculated for a set of different rates of pure QD dephasing [13], γ_d, which causes a reduction of the transmission dips before and after the peak. Pure dephasing also causes a blurring of the spectral normal mode splitting [13], which in turn raises the transmission for increasing γ_d. (c) Pump-power dependence of the cavity transmission for coincident pulses repeating at 80 MHz. Different curves correspond to the average power of each of the pulses used in the experiment (averaged over 13 ns, the pulse repetition period). (d) Signal observed when the cavity-QD system is probed with two 40 ps long pulses as a function of their delay. When the two pulses have a temporal overlap inside the cavity (i.e., delay approaches zero), the QD saturates and the overall cavity transmission increases. The power in the single of the two pulses corresponds roughly to the 3.4 nW trace in (c). Best agreement is found with the theoretical plot for a pure dephasing rate $\gamma_d/2\pi \sim 5$ GHz (the solid red line).

This experiment is performed on a different QD-cavity system with similar parameters $\{\kappa, g, \gamma\}/2\pi = \{27.2, 21.2, 1\}$ GHz while the temperature of the system is kept at 38 K. Photon statistics measurements on the system showed nonclassical behavior confirming only a single QD is coupled to the cavity and results in the effects of photon blockade and photon induced tunneling, confirming the quantum nature of the system (see Supplemental Material [10] and Ref. [15]). Figure 3(c) plots the time-averaged cavity transmitted signal observed on a spectrometer for coincident pump pulses with an average power of both pulses increasing from 0.3 to 9.2 nW before the objective lens. It is evident that for powers beyond ~9 nW, the polariton mode splitting disappears as the QD is saturated. This suggests that the QD-cavity system acts as a highly nonlinear system that increases its transmission for coincident pulses. Based on the result of Fig. 3(c), we choose average powers of individual pulses to be 3.4 nW, as it is evident that the presence of two such pulses saturates the system leading to maximum cavity transmission. This pulse power corresponds to an intracavity photon number of 0.4 for each pulse ($\eta = 3\%$). Then we perform the optical switching experiment by tuning the delay between two such pulses, as shown in Fig. 3(d): the cavity transmission rises by 22% when the pulses are coincident at $\Delta t = 0$. This transmission peak agrees with the theoretical prediction as shown by the red curve. In the theory plot, we also observe reduced transmission at a nonzero time delay. We find that by including a pure QD dephasing term into the master equation model, the transmission dips are diminished [Fig. 3(b)], as observed in the experimental results. The best fit to experimental data is found for a dephasing rate of $\gamma_d/2\pi \approx 5$ GHz.

In conclusion, we demonstrated the ultrafast all-optical switching between the pulsed control beam and a CW or pulsed signal beam via a strongly coupled QD/cavity system. A strong nonlinear response exists at low powers corresponding to mean intracavity photon numbers below one. The large nonlinearity may be of use in classical all-optical signal processing [2]—for example, for the implementation of all-optical logic gates operating at the single- or few-photon level. In addition, it may be beneficial for quantum information processing with optical nonlinearities [16–19]. Moreover, the QD-cavity system is ideal for on-chip integration and can easily operate with repetition rates up to tens of GHz.

Financial support was provided by the Office of Naval Research, National Science Foundation, and Army Research Office. A. M. was supported by the SGF. Work was performed in part at the Stanford Nanofabrication Facility of NNIN supported by the National Science Foundation. D. E. acknowledges support by the Sloan Foundation and by the U.S. Air Force Office of Scientific Research Young Investigator Program, AFOSR Grant No. FA9550-11-1-0014, supervised by Dr. Gernot Pomrenke. J. Vuckovic would also like to acknowledge support from the Alexander von Humboldt Foundation.

Note added.—After submitting this Letter, we learned about a related experiment performed by another group [20].

*englund@columbia.edu
†arkam@stanford.edu

[1] *Optical Computing*, edited by F. A. P. Tooley and B. S. Wherrett, Scottish Graduate Series (IOP Publishing Ltd., Bristol, U.K., 1989).
[2] H. Mabuchi, Phys. Rev. A **80**, 045802 (2009).
[3] M. Bajcsy, S. Hofferberth, V. Balic, T. Peyronel, M. Hafezi, A. S. Zibrov, V. Vuletic, and M. D. Lukin, Phys. Rev. Lett. **102**, 203902 (2009).
[4] D. Englund, A. Faraon, I. Fushman, N. Stoltz, P. Petroff, and J. Vučković, Nature (London) **450**, 857 (2007).
[5] K. Srinivasan and O. Painter, Nature (London) **450**, 862 (2007).
[6] I. Fushman, D. Englund, A. Faraon, N. Stoltz, P. Petroff, and J. Vuckovic, Science **320**, 769 (2008).
[7] Y. Akahane, T. Asano, B.-S. Song, and S. Noda, Nature (London) **425**, 944 (2003).
[8] M. Toishi, D. Englund, A. Faraon, and J. Vučković, Opt. Express **17**, 14 618 (2009).
[9] A. Majumdar *et al.*, Phys. Rev. B **82**, 045306 (2010).
[10] See Supplemental Material at http://link.aps.org/supplemental/10.1103/PhysRevLett.108.093604 for our observations of nonclassical light statistics (second order autocorrelation function $g^2(0) > 1$ in the tunneling and $g^2(0) < 1$ in the blockade regime) from the cavity-transmitted light.
[11] M. Winger *et al.*, Phys. Rev. Lett. **103**, 207403 (2009).
[12] D. A. B. Miller, in *Digital Optical Computing*, edited by R. A. Athale, SPIE Critical Reviews of Optical Science and Technology Vol. CR35 (SPIE-International Society for Optical Engineering, Bellingham, WA, 1990), pp. 68–76.
[13] D. Englund, A. Majumdar, A. Faraon, T. Mitsuru, N. Stoltz, P. Petroff, and J. Vuckovic, Phys. Rev. Lett. **104**, 073904 (2010).
[14] A. Majumdar *et al.*, Opt. Express **18**, 3974 (2010).
[15] A. Majumdar *et al.*, arXiv:1106.1926.
[16] W. J. Munro *et al.*, Phys. Rev. A **71**, 033819 (2005).
[17] Q. A. Turchette, C. J. Hood, W. Lange, H. Mabuchi, and H. J. Kimble, Phys. Rev. Lett. **75**, 4710 (1995).
[18] I. L. Chuang and Y. Yamamoto, Phys. Rev. A **52**, 3489 (1995).
[19] N. Imoto, H. A. Haus, and Y. Yamamoto, Phys. Rev. A **32**, 2287 (1985).
[20] D. Sridharan *et al.*, arXiv:1107.3751v1.